Biochimica et Biophysica Acta 1794 (2009) 689–697

Contents lists available at ScienceDirect

Biochimica et Biophysica Acta

journal homepage: www.elsevier.com/locate/bbapap

New oxidase from *Bjerkandera* arthroconidial anamorph that oxidizes both phenolic and nonphenolic benzyl alcohols

Elvira Romero, Patricia Ferreira [1], Ángel T. Martínez, María Jesús Martínez *

Centro de Investigaciones Biológicas, CSIC, Ramiro de Maeztu 9, E-28040 Madrid, Spain

ARTICLE INFO

Article history:
Received 21 October 2008
Received in revised form 17 November 2008
Accepted 18 November 2008
Available online 6 December 2008

Keywords:
Flavoenzyme
Benzyl alcohol
Hydroxybenzyl alcohol
Aromatic aldehyde
Aryl-alcohol oxidase
Vanillyl-alcohol oxidase

ABSTRACT

A new flavooxidase is described from a *Bjerkandera* arthroconidial anamorph. Its physicochemical characteristics, a monomeric enzyme containing non-covalently bound flavin adenine dinucleotide (FAD), and several catalytic properties, such as oxidation of aromatic and polyunsaturated aliphatic primary alcohols, are similar to those of *Pleurotus eryngii* aryl-alcohol oxidase (AAO). However, it also efficiently oxidizes phenolic benzyl and cinnamyl alcohols that are typical substrates of vanillyl-alcohol oxidase (VAO), a flavooxidase from a different family, characterized by its multimeric nature and presence of covalently-bound FAD. The enzyme also differs from *P. eryngii* AAO by having extremely high efficiency oxidizing chlorinated benzyl alcohols (1000–1500 s^{-1} mM^{-1}), a feature related to the different alcohol metabolites secreted by the *Pleurotus* and *Bjerkandera* species including chloroaromatics, and higher activity on aromatic aldehydes. What is even more intriguing is the fact that, the new oxidase is optimally active at pH 6.0 on both *p*-anisyl and vanillyl alcohols, suggesting a mechanism for phenolic benzyl alcohol oxidation that is different from that described in VAO, which proceeds via the substrate phenolate anion formed at basic pH. Based on the above properties, and its ADP-binding motif, partially detected after N-terminus sequencing, the new enzyme is classified as a member of the GMC (glucose–methanol–choline oxidase) oxidoreductase family oxidizing both AAO and VAO substrates.

1. Introduction

White-rot fungi are able to degrade the recalcitrant and heterogeneous lignin polymer using an unspecific oxidative system that involves extracellular peroxidases, oxidases, laccases, and low molecular-mass compounds [1]. Lignin degradation leads to the formation of a broad spectrum of simple aromatic products, and similar compounds can also be synthesized *de novo* by some ligninolytic basidiomycetes [2,3]. Among them, aryl alcohols and aldehydes participate in cyclic redox reactions catalyzed by aryl-alcohol oxidases (AAO) and aryl-alcohol dehydrogenases (AAD) resulting in continuous generation of H_2O_2 from O_2 reduction, as described in *Pleurotus eryngii* [4].

H_2O_2 generated by AAO and other basidiomycete oxidases – such as glyoxal oxidase (a copper radical oxidase), pyranose-2 oxidase and methanol oxidase (two flavooxidases as AAO) [5–7] – plays a key role in lignin degradation as the oxidizing substrate of ligninolytic peroxidases, and also reacts with ferrous iron generating the hydroxyl free radical involved in the initial wood decay by different wood-rotting fungi [8,9]. Moreover, it has also been reported that *Pleurotus ostreatus* AAO (described initially as veratryl alcohol oxidase) prevents repolymerization reactions during lignin degradation [10].

AAO was first reported in *Polystictus versicolor* (a synonym of *Trametes versicolor*) [11] and then in other ligninolytic basidiomycetes from the genera *Pleurotus* [12–15] and *Bjerkandera* [16] although the latter was not thoroughly characterized. In these fungi AAO are monomeric glycoproteins of 71–81 kDa with dissociable FAD as a cofactor. AAO efficiently oxidizes non-phenolic aryl alcohols with a primary hydroxyl in Cα, but is inactive with respect to aliphatic saturated alcohols. A comprehensive substrate specificity study of *P. eryngii* AAO revealed that the enzyme also acted on aliphatic polyunsaturated alcohols and showed residual activity on aromatic aldehydes [17]. Other AAO with partially different catalytic properties have also been found in *Phanerochaete chrysosporium* mycelium [18] and in some ascomycetous fungi [19].

Vanillyl-alcohol oxidase (VAO) also oxidizes benzylic alcohols to the corresponding aldehydes reducing O_2 to H_2O_2 but, in contrast to AAO, it only acts on vanillyl alcohol and other phenolic benzyl

Abbreviations: AAD, aryl-alcohol dehydrogenase; AAO, aryl-alcohol oxidase; ABTS, 2,2′-azino-bis(3-ethylbenzothiazoline-6-sulfonic acid); Endo H, endoglycosidase H; FAD, flavin adenine dinucleotide; GMC, glucose–methanol–choline oxidase; HRP, horseradish peroxidase; k_{cat}, maximal turnover number; K_i, inhibition constant; K_m, Michaelis constant; MALDI, matrix-assisted laser desorption/ionization; p*I*, isoelectric point; SDS-PAGE, sodium dodecyl sulfate-polyacrylamide gel electrophoresis; TOF, time of flight; U, enzyme unit; VAO, vanillyl-alcohol oxidase

* Corresponding author. CIB, CSIC, Ramiro de Maeztu 9, E-28040 Madrid, Spain. Tel.: +34 918373112; fax: +34 915360432.
E-mail address: mjmartinez@cib.csic.es (M.J. Martínez).
[1] Present address: Departamento de Bioquímica y Biología Molecular y Celular, Facultad de Ciencias, Universidad de Zaragoza, E-50009 Zaragoza, Spain.

1570-9639/$ – see front matter © 2008 Elsevier B.V. All rights reserved.
doi:10.1016/j.bbapap.2008.11.013

alcohols, and also catalyzes deamination, hydroxylation and demethylation reactions [20]. VAO was described in the ascomycetous fungus *Penicillium simplicissimum* [21]. This intracellular flavoprotein is a homooctamer with each 64 kDa monomer containing a covalently-bound FAD [22]. Homodimeric VAO has been described in the ascomycete *Byssochlamys fulva* [23].

A *Geotrichum*-type arthroconidial fungus was isolated by the authors from a deteriorated compact disc found in Belize (Central America) [24]. Further studies revealed that the isolate was an anamorph of the white-rot fungus *Bjerkandera adusta* according to the sequence of the internal transcribed spacer region of its ribosomal DNA, morphological features, and production of ligninolytic enzymes [25]. In the present paper, we report the purification and characterization of an H_2O_2-generating extracellular oxidase produced by this fungus, which shares catalytic properties with both *P. eryngii* AAO and *P. simplicissimum* VAO.

2. Materials and methods

2.1. Chemicals and enzymes

m-Anisyl, *p*-anisyl, benzyl, *m*-chlorobenzyl, *p*-chlorobenzyl, cinnamyl, coniferyl, *m*-fluorobenzyl, *p*-fluorobenzyl, isovanillyl, vanillyl and veratryl alcohols, methanol, 2,4-hexadien-1-ol, eugenol, 4-(methoxymethyl)phenol, *p*-anisaldehyde, 3-chloro-*p*-anisaldehyde, *m*-chlorobenzaldehyde, *trans*-cinnamaldehyde, *m*-fluorobenzaldehyde, *p*-nitrobenzaldehyde, vanillin, benzyl-methyl ether, 4-methoxybenzylamine, and 3-chloro-*p*-anisic, *m*-chlorobenzoic, *m*-fluorobenzoic and *p*-nitrobenzoic acids, methanol oxidase (from *Pichia pastoris*), and glucose oxidase (from *Aspergillus niger*; type II) were obtained from Sigma-Aldrich. 3-Chloro-*p*-anisyl alcohol was synthesized by borane-tetrahydrofuran reduction of the corresponding acid [26] at the Instituto de Ciencia de Materiales de Aragón (CSIC, Zaragoza, Spain). Amplex® Red (10-acetyl-3,7-dihydroxyphenoxazine) was from Invitrogen. 2,2′-Azino-bis(3-ethylbenzothiazoline-6-sulfonic acid) (ABTS), endoglycosidase H (Endo H), and horseradish peroxidase (HRP) were from Roche.

2.2. Fungus and culture conditions

The *B. adusta* anamorph is deposited in the IJFM culture collection of the CIB (CSIC, Madrid, Spain) as A757, and the sequences of the ribosomal internal transcribed spacers and the 5.8S DNA gene are available from GenBank® under accession number EF441742 [25]. The fungus was grown in glucose-peptone-yeast extract medium [27] at 28 °C and 150 rpm.

2.3. Enzyme purification

After 7-d incubation, mycelium was removed by filtration and the culture was concentrated and dialyzed against 10 mM sodium acetate, pH 5.5, by ultrafiltration (Filtron; 3 kDa cut-off). The concentrate was loaded into a 5 ml HiTrap Q FF column (GE Healthcare) and the retained proteins eluted with a 0–250 mM NaCl gradient (140 min, 1 ml/min). The active fractions were pooled, concentrated and dialyzed against the above buffer, pH 5.0, in a stirred cell (Amicon; 3 kDa cut-off). The desalted sample was loaded onto an anion-exchange Mono Q HR 5/5 column (Pharmacia) equilibrated with the same buffer, and eluted using a 0–200 mM NaCl gradient (43 min, 0.8 ml/min). Fractions containing oxidase activity were collected, concentrated in a centrifugal filter (Millipore; 5 kDa cut-off) and loaded onto a gel permeation Superdex-75 HR 10/30 column (Pharmacia LKB, HR) with the same buffer containing 150 mM NaCl (0.4 ml/min). Low Molecular Weight Gel Filtration Calibration Kit (Pharmacia) was used for determination of molecular mass. Aliquots of purified enzyme were stored at −80 °C. The protein amount after each purification step was determined using the Bio-Rad Assay with bovine serum albumin as a standard.

2.4. Electronic absorption spectrum and molar extinction coefficient

UV–visible spectra of the purified enzyme, and the released FAD cofactor after heat denaturation (5 min, 80 °C), were recorded at 24 °C in 10 mM sodium phosphate, pH 6.0, in a Hewlett–Packard 8453 diode-array spectrophotometer. The enzyme extinction coefficient was determined using the following equation:

$$\varepsilon_{463} = \varepsilon_{FAD} \cdot A_{463}/A_{450} \quad (1)$$

where A_{463} is the enzyme absorbance at 463 nm, A_{450} is the free-FAD absorbance at 450 nm, and ε_{FAD} is the free-FAD extinction coefficient at 450 nm (11,300 M^{-1} cm^{-1}). Enzyme concentration was then estimated from its A_{463}.

2.5. Electrophoresis and isoelectric focusing

Aliquots were analyzed by 7.5% sodium dodecyl sulfate-polyacrylamide gel electrophoresis (SDS-PAGE) on a Mini Protean III Cell (Bio-Rad) (120 V, pH 8.5 and 24 °C) after each purification step and from deglycosylated enzyme, obtained by overnight incubation of 5 μg of enzyme with 15 mU of Endo H at 37 °C in 10 mM sodium phosphate (pH 6.0). Silver technique was used for protein staining, and high-molecular-weight standard mixture (Bio-Rad) was run in parallel for calibration.

The isoelectric point (p*I*) before and after deglycosylation was determined on 5% polyacrylamide gel (pH range of 2.8–6.7) using the horizontal Model 1405 Electrophoresis Cell (Bio-Rad) (3 h at 1000 V, 5 mA, 5 W and 24 °C). The anode and cathode solutions were 1 M H_3PO_4 and 1 M NaOH, respectively. The pH gradient was measured using a contact electrode, and the p*I* was determined by interpolation. The focused proteins were stained with Coomassie blue R-250, and for activity a solution containing 10 mM veratryl alcohol, 10 mM NaOH, 3 M IK and 60 mM starch was used [28].

2.6. Matrix-assisted laser desorption/ionization-time of flight (MALDI-TOF) mass spectrometry

Molecular masses were determined with an Autoflex III MALDI-TOF-TOF instrument (Bruker) equipped with a smartbeam laser. One μl of a mixture (1:1, v/v) of protein solution (1 μg/μl) and matrix solution (saturated sinapic acid in acetonitrile/0.1% trifluoroacetic acid 1:2, v/v) was spotted on a stainless steel target and dried at 24 °C. Spectra were acquired using a laser power just above the ionization threshold. Samples were analyzed in the positive ion detection and delayed extraction linear mode. Typically, 1000 laser shots were summed into a single mass spectrum. Protein calibration standard II (Bruker) was used for external calibration.

2.7. N-terminal sequence

The N-terminal sequence was determined by automatic Edman degradation of 100 pmol of protein using a Procise 494 sequencer (Perkin Elmer). Sequence alignments were produced with CLUSTAL W of SDSC Biology Workbench [29].

2.8. Activity assay and steady-state kinetics

The enzymatic assays described below were performed in a Shimadzu UV-160 spectrophotometer at 24 °C in 100 mM sodium phosphate, pH 6.0 (unless otherwise stated). For curve fitting the program SigmaPlot 11.0 was used. Standard enzyme activity was measured by monitoring the oxidation of 10 mM veratryl alcohol to veratraldehyde (ε_{310}, 9300 M^{-1} cm^{-1}) [17]. Activity was expressed as

Table 1
Purification of the new oxidase from the *B. adusta* anamorph

Purification step	Total activity (U)	Total protein (mg)	Specific activity (U mg^{-1})	Yield (%)	Purification (fold)
Culture	534	85.7	6.2	100.0	1.0
HiTrap Q FF	531	20.8	25.5	99.5	4.1
Mono Q	395	12.6	31.3	74.3	5.0
Superdex-75	245	5.5	44.8	62.0	7.2

Enzymatic activity was estimated with 10 mM veratryl alcohol (pH 6.0) and protein content using the Bio-Rad Protein Assay.

international units (U), defined as the amount of enzyme that releases 1 μmol product/min^{-1}.

Steady-state kinetic constants for oxidation of different alcohols to the corresponding aldehydes were determined by fitting initial reaction rates at different substrate concentrations (S) to Eqs. 2 and 3, where K_m represents the Michaelis constant, k_{cat} the maximal turnover number and k_{cat}/K_m is the catalytic efficiency of the enzyme.

$$v = \frac{k_{cat}S}{K_m + S} \tag{2}$$

$$v = \frac{(k_{cat}/K_m)S}{1 + (k_{cat}/K_m)S/k_{cat}} \tag{3}$$

Molar absorption coefficients of benzaldehyde (ε_{250}, 13,800 M^{-1} cm^{-1}), *m*-anisaldehyde (ε_{314}, 2540 M^{-1} cm^{-1}) and *p*-anisaldehyde (ε_{285}, 16,950 M^{-1} cm^{-1}) were from Guillén et al. [17], those of *m*-chlorobenzaldehyde (ε_{240}, 5923 M^{-1} cm^{-1}), *p*-chlorobenzaldehyde (ε_{260}, 15,862 M^{-1} cm^{-1}), cinnamaldehyde (ε_{310}, 15,600 M^{-1} cm^{-1}), *m*-fluorobenzaldehyde (ε_{246}, 10,280 M^{-1} cm^{-1}), *p*-fluorobenzaldehyde (ε_{252}, 13,700 M^{-1} cm^{-1}), 2,4-hexadien-1-al (ε_{280}, 30,140 M^{-1} cm^{-1}), isovanillin (ε_{307}, 7383 M^{-1} cm^{-1}) and vanillin (ε_{309}, 8332 M^{-1} cm^{-1}) were from Ferreira et al. [30], and that of 3-chloro-*p*-anisaldehyde (ε_{295}, 15,000 M^{-1} cm^{-1}) was from de Jong et al. [31]. The molar absorption coefficient of coniferaldehyde (ε_{338}, 24,222 M^{-1} cm^{-1}) was calculated using a commercial standard.

Methanol oxidase activity was tested by coupled assay with HRP resulting in ABTS oxidation to its cation radical (ε_{405}, 36,800 M^{-1} cm^{-1}). The reaction mixture contained 0.033% [v/v] methanol, 2 mM ABTS and 0.83 U/ml HRP (pH 6.0 and 7.5). Commercial methanol oxidase from *P. pastoris* was used as a control.

The oxidation of aromatic aldehydes to the corresponding acids was first monitored by spectral changes using 0.3 mM *m*-chlorobenzaldehyde, 0.2 mM *m*-fluorobenzaldehyde, and 0.1 mM 3-chloro-*p*-anisaldehyde, *p*-nitrobenzaldehyde, *p*-anisaldehyde, *trans*-cinnamaldehyde, vanillin and 0.5 μM enzyme, at pH 6.0 and 24 °C. Steady-state kinetic constants for aldehyde oxidation were calculated by H_2O_2 production using an HRP coupled assay with Amplex® Red as the final substrate, at pH 6.0 and 25 °C. HRP (6 U/ml) oxidizes Amplex® Red (58 μM) in the presence of H_2O_2 generating the fluorescent resorufin (ε_{563} 52,000 M^{-1} cm^{-1}) [32].

Possible demethylation, hydroxylation and deamination reactions were investigated using 9 mM benzyl-methyl ether or 1.5 mM 4-(methoxymethyl)phenol, 1 mM eugenol and 1.5 mM 4-methoxybenzylamine respectively, at pH 6.0 and 7.5. The assays were initiated by adding 0.5 μM oxidase and subsequently studying spectral changes. Eugenol (2 and 6 μM), benzyl-methyl ether (83 and 166 μM), 4-(methoxymethyl)phenol (300 and 900 μM), 4-methoxybenzylamine (4 and 8 mM), and methanol (1 and 2 M) were also evaluated as inhibitors of veratryl alcohol oxidation at pH 6.0 (and pH 8.0 in the case of 4-methoxybenzylamine). Inhibition constants (K_i) were determined by nonlinear fitting of data at the different inhibitor concentrations (I) to Eq. 4 for competitive inhibition or Eq. 5 for non-competitive inhibition.

$$v = \frac{k_{cat}S}{K_m\left(1 + \frac{I}{K_i}\right) + S} \tag{4}$$

$$v = \frac{k_{cat}S}{K_m\left(1 + \frac{I}{K_i}\right) + S\left(1 + \frac{I}{K_i}\right)} \tag{5}$$

2.9. Anaerobic reduction of the enzyme by alcohol substrates

Aliquots (1–4 μl) of 0.7 mM *p*-anisyl alcohol or 0.6 mM vanillyl alcohol were anaerobically added to a solution of oxidase (22 μM) in 100 mM sodium phosphate, pH 6.0. The redox state of the flavin was monitored spectrophotometrically at every substrate concentration. All solutions were flushed with argon and contained 310 mM glucose and 1 U glucose oxidase to ensure anaerobic conditions.

2.10. Effect of pH and temperature on enzyme activity and stability

The pH dependence of the steady-state kinetic parameters with *p*-anisyl and vanillyl alcohols as substrates was determined from pH 2.5 to 5.0 in 100 mM citrate phosphate buffer, from pH 6.0 to 8.0 in 100 mM sodium phosphate buffer, and at pH 8.5 in 100 mM sodium pyrophosphate buffer. The kinetic constants were estimated from initial velocities taking linear increments. The pH profiles of the k_{cat}/K_m values were determined by fitting experimental data to Eq. 6, which

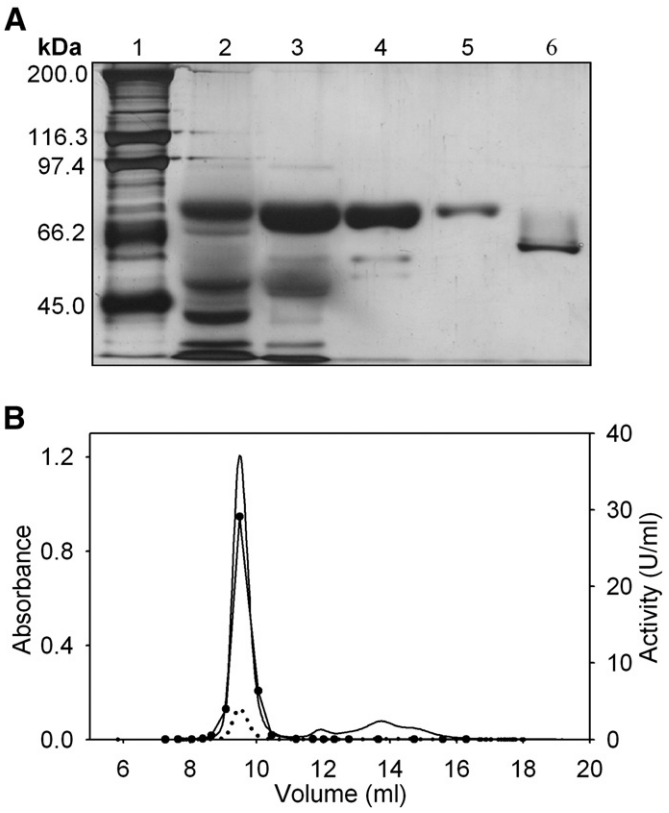

Fig. 1. SDS-PAGE during purification of the new oxidase (A), and pure enzyme elution from Superdex-75 (B). (A) Silver-stained gel (7.5%) from samples after the different purification steps: lane 1, molecular weight markers; lane 2, crude extract; lane 3, HiTrap Q; lane 4, Mono Q; lane 5, Superdex-75; lane 6, deglycosylated protein after Superdex-75. (B) Absorption at 280 nm (—) and 465 nm (····), and oxidase activity against veratryl alcohol (–●–) in the last purification step.

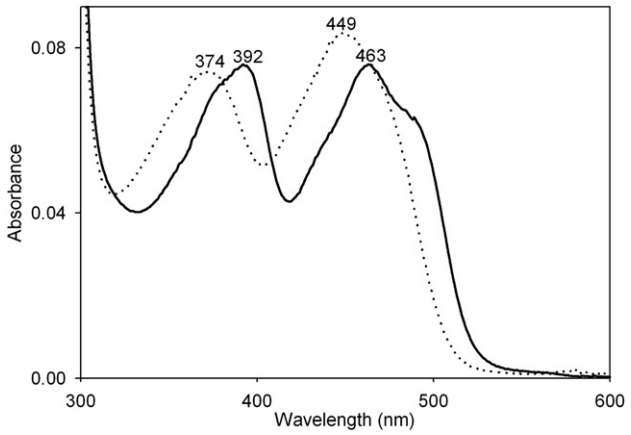

Fig. 2. Electronic absorption spectra of the new oxidase, before (—) and after heat denaturation (·····). The spectra were collected from enzyme solution (7.3 μM) in 10 mM sodium phosphate, pH 6.0, and from the same sample after 5 min heating at 80 °C resulting in the release of the FAD cofactor with slightly different spectroscopic properties.

describes a curve composed of linear regions of slopes +1, 0, and −1, where K_1 and K_2 are the dissociation constants for ionization of groups that must be unprotonated and protonated for catalysis respectively, C is the pH-independent value of the kinetic parameter of interest, and H is H^+ concentration.

$$\log Y = \log \frac{C}{1 + H/K_1 + K_2/H} \quad (6)$$

pH stability was estimated by measuring the remaining oxidase activity during a 24-h incubation in 100 mM citrate–phosphate–borate, pH 2.0–9.0, at 24 °C, using the standard assay.

Optimal temperature was evaluated by the standard assay on a Cary 4000 UV–vis spectrophotometer equipped with a temperature control unit (4–55 °C). For the thermostability study, aliquots were assayed for enzymatic activity during 24 h at 25–50 °C in 100 mM sodium phosphate, pH 6.0.

3. Results

3.1. Purification and physicochemical characterization of the B. adusta anamorph oxidase

An oxidase acting on benzyl alcohols was purified from glucose–peptone–yeast extract cultures of an arthroconidial *B. adusta* anamorph.

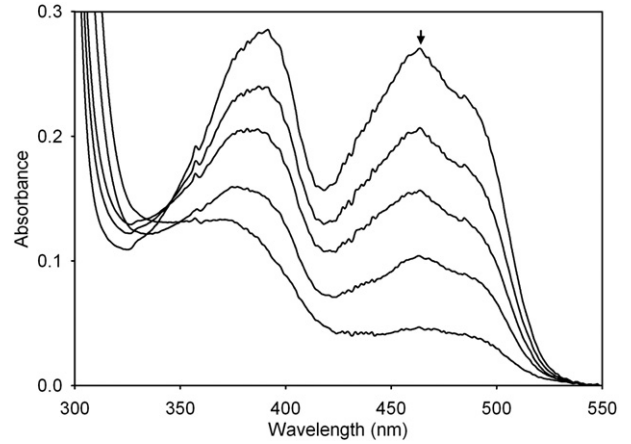

Fig. 3. Anaerobic reduction of the new oxidase by *p*-anisyl alcohol. Titration experiments were conducted under anaerobic conditions using 22 μM oxidase in 100 mM sodium phosphate, pH 6.0, at 24 °C. Spectra were recorded in the presence of 0, 7, 14, 28, 56 μM *p*-anisyl alcohol. Arrow indicates the direction of the spectral changes.

Table 2
Steady-state kinetic constants of the new oxidase for different alcohols

		K_m (μM)	k_{cat} (s^{-1})	k_{cat}/K_m (s^{-1} mM^{-1})
Benzyl	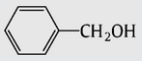	329±15	6±0.1	18±1
m-Anisyl	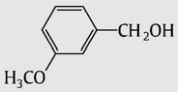	156±5	54±0.4	349±8
p-Anisyl	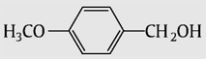	187±16	121±2	646±45
Veratryl	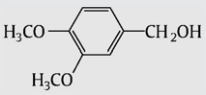	2094±114	47±1	22±1
m-Chlorobenzyl	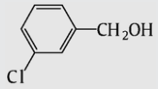	23±1	24±0.2	1052±29
p-Chlorobenzyl	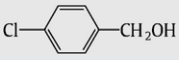	71±4	26±0.3	361±15
3-Chloro-*p*-anisyl	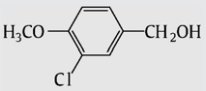	49±4	73±2	1480±114
m-Fluorobenzyl	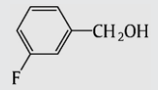	208±11	10±0.1	47±2
p-Fluorobenzyl	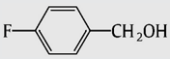	408±47	9±0.3	22±2
Isovanillyl	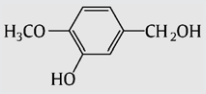	1115±35	56±1	51±1
Vanillyl	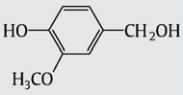	1404±77	44±1	31±1
Cinnamyl	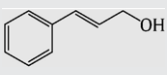	73±3	22±0.3	305±11
Coniferyl	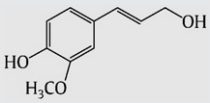	1860±124	9±0.3	5±0.2
2,4-Hexadien-1-ol	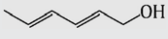	521±27	97±2	186±7

All experiments were performed at 24 °C in 100 mM sodium phosphate, pH 6.0. Mean and standard errors were obtained by fitting experimental data to a hyperbolic Michaelis–Menten function.

The purification process (Table 1) included three chromatographic steps with a final yield of over 60% of the initial activity. Fractions with oxidase activity were separated from most contaminating proteins during the first chromatographic step (Fig. 1A, lane 3) but two additional chromatographies using Mono Q and Superdex-75 (Fig. 1B) were necessary to yield electrophoretically-homogeneous protein (Fig. 1A, lane 5).

SDS-PAGE showed that the enzyme, with a molecular mass around 76 kDa, is a major protein in the fungal culture (Fig. 1A, lane 2). The increased electrophoretic mobility after Endo H treatment (Fig. 1A, lanes 5 and 6) indicated 7.4% of *N*-linked carbohydrate. The molecular masses from MALDI-TOF mass spectrometry (76.069 kDa) and calibrated gel-permeation (72 kDa) confirmed that it is a monomeric protein. Isoelectric focusing generally revealed a single band with a p*I* of 4.45. Two bands with similar p*I* were detected in some samples, but they were reduced to a single band after Endo H treatment. The N-terminal sequence obtained for the new oxidase was ATFFTDASQLPATVYDFIVVG.

The oxidase was stable for 24 h at pH 4.0–6.0. Its activity decreased to 27% after 24 h at pH 7.0. At more acidic/basic pH, it was drastically reduced after a short incubation. The effect of pH on the catalytic efficiency of the enzyme is discussed below. With regard to temperature, it had the highest activity (pH 6.0) at 45 °C. Moreover, it was stable for 24 h at 25 °C, and retained 40% activity after 4 h at 40 °C (above this temperature activity was quickly lost).

3.2. Flavoenzyme spectrum and anaerobic reduction of flavin

UV–visible spectra showed two peaks (at 392 and 463 nm) characteristic of FAD-containing proteins in the oxidized state, and an A_{280}/A_{463} ratio of 10. The flavin cofactor was released when the enzyme was heat treated (Fig. 2). This revealed that it was not covalently linked, and allowed us to calculate an enzyme ε_{463} of 10,932 M^{-1} cm^{-1}.

Anaerobic reduction with *p*-anisyl alcohol showed that the flavin is converted to a two-electron reduced form upon incubation with a 2.5-fold substrate concentration (Fig. 3) and similar results were obtained with a 3.5-fold concentration of vanillyl alcohol (data not shown). These reactions were immediately reversible after aeration of the samples. During reduction with both substrates, stoichiometric amounts of *p*-anisaldehyde and vanillin were produced (determined from absorbances at 298 nm and 309 nm, respectively).

3.3. Substrate specificity of the new oxidase

Several phenolic and non-phenolic benzyl and cinnamyl alcohols, and the aliphatic 2,4-hexadien-1-ol and methanol were investigated as substrates of the oxidase from the *B. adusta* anamorph, together with other VAO substrates. Table 2 shows the steady-state kinetic constants monitored at the wavelengths of the aldehyde products. The

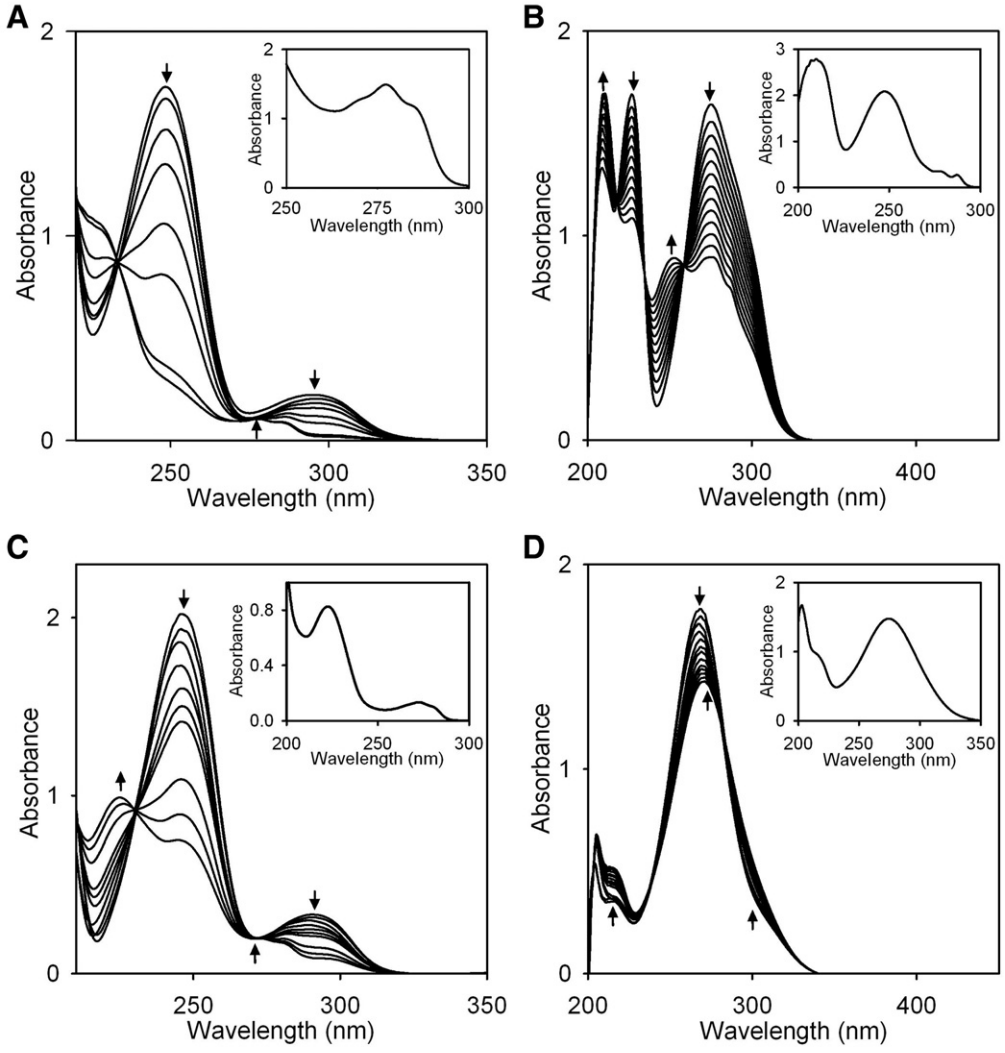

Fig. 4. Electronic absorption spectra during oxidase conversion of 0.3 mM *m*-chlorobenzaldehyde (A), 0.1 mM 3-chloro-*p*-anisaldehyde (B), 0.2 mM *m*-fluorobenzaldehyde (C) and 0.1 mM *p*-nitrobenzaldehyde (D). Spectra were recorded at 0, 1, 5, 10, 20, 30, 60 and 120 min (A), every 2 h during 24 h (B), at 0, 0.5, 1, 2, 3, 4, 5, 10, 15 and 24 h (C), or every 4 h during 48 h (D). All reactions contained 0.5 μM enzyme in 100 mM sodium phosphate, pH 6.0, at 24 °C. Reference spectra of 2.5 mM *m*-chlorobenzoic, 0.2 mM 3-chloro-*p*-anisic, 0.1 mM *m*-fluorobenzoic and 0.2 mM *p*-nitrobenzoic acids are shown in the corresponding insets. Arrows indicate the direction of the spectral changes.

Table 3
Steady-state kinetic constants of the new oxidase for different aldehydes

		K_m (μM)	k_{cat} (s^{-1})	k_{cat}/K_m (s^{-1} mM^{-1})
m-Chlorobenzaldehyde	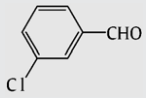	176±14	0.2±0.005	1±0.09
3-Chloro-*p*-anisaldehyde	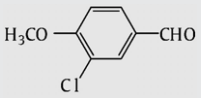	48±3	0.002±0.00003	0.05±0.002
m-Fluorobenzaldehyde	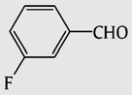	258±15	0.01±0.0002	0.05±0.002
p-Nitrobenzaldehyde	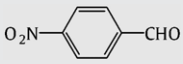	380±22	0.004±0.00006	0.01±0.001

All experiments were performed at 24 °C in 100 mM sodium phosphate, pH 6.0. Mean and standard errors were obtained by fitting experimental data to a hyperbolic Michaelis–Menten function.

enzyme had catalytic efficiency oxidizing 3-chloro-*p*-anisyl>*m*-chlorobenzyl>*p*-anisyl>*p*-chlorobenzyl>*m*-anisyl>cinnamyl>2,4-hexadien-1-ol, with k_{cat}/K_m values over 180 s^{-1} mM^{-1} in all the cases. Its outstanding efficiency, oxidizing the two former substrates (with values of over 1000 s^{-1} mM^{-1}), is due to high affinity. The above substrates also showed some of the highest turnover numbers, with k_{cat} values always over 20 s^{-1}, although the order was different: *p*-anisyl>2,4-hexadien-1-ol>3-chloro-*p*-anisyl>*m*-anisyl>*p*-chlorobenzyl>*m*-chlorobenzyl>cinnamyl. High turnover numbers were also found for veratryl, vanillyl and isovanillyl alcohols (k_{cat}, 40–60 s^{-1}) although the enzyme had low affinity for these three substrates, which yielded the highest K_m values together with coniferyl alcohol. The highest activity, up to 20-fold compared with benzyl alcohol, was obtained with the methoxylated substrates (including *p*-anisyl alcohol). By contrast, the chlorine and fluorine substituents caused a more modest or null effect on k_{cat}. Regarding polyunsaturated aliphatic alcohols, the enzyme was able to oxidize 2,4-hexadien-1-ol, with efficiency and k_{cat} values 10 and 16-fold higher, respectively, than those of benzyl alcohol. Methanol was not oxidized. Finally, the enzyme also oxidized the two phenolic benzyl alcohols assayed (vanillyl and isovanillyl alcohols) with higher (over 7-fold) k_{cat} than benzyl alcohol. However, phenolic coniferyl alcohol was the worst substrate assayed as revealed by the low catalytic efficiency constant.

In addition to oxidizing aromatic, and polyunsaturated aliphatic, alcohols the enzyme also exhibited aromatic-aldehyde oxidase activity, converting the aldehydes to the corresponding acids (Fig. 4). Table 3 shows the steady-state kinetic constants for the best aldehyde substrates, estimated from the H_2O_2 released using the HRP coupled assay. The enzyme had catalytic efficiency oxidizing *m*-chlorobenzaldehyde>*m*-fluorobenzaldehyde>3-chloro-*p*-anisaldehyde>*p*-nitrobenzaldehyde, with k_{cat}/K_m values up to 1.3 $s^{-1}mM^{-1}$. The lower efficiency oxidizing the above aldehydes is due to a reduced turnover number (k_{cat}, 0.002–0.23 s^{-1}), since the affinity was in the same range as that found for many of the alcohol substrates (K_m 48–380 μM). No oxidation of vanillin was detected, and *p*-anisaldehyde and cinnamaldehyde were very poor substrates.

3.4. pH dependence of catalytic activity

The pH dependence of the steady-state kinetic parameters with *p*-anisyl or vanillyl alcohols as substrates was determined in the pH range from 2.5 to 8.5 (the enzyme was not stable at more extreme pH values). As shown in Fig. 5, the k_{cat}/K_m *vs* pH profiles for both substrates were bell-shaped, and only a little wider in the case of *p*-anisyl alcohol, which was consistent with the involvement of two ionizable groups in the catalysis. The pK_a values (from Eq. 6) for *p*-anisyl alcohol (2.17±0.08 and 8.65±0.06) were similar to those for vanillyl alcohol (2.34±0.05 and 8.15±0.03).

3.5. Some inhibitors of the oxidase activity

Other oxidative reactions reported for VAO were finally tested (by following eventual spectral changes) but the enzyme was not able to catalyze demethylation of benzyl-methyl ether or 4-(methoxymethyl) phenol, hydroxylation of eugenol, or deamination of 4-methoxybenzylamine (at pH 6.0 or 7.5). However, these compounds caused competitive inhibition at pH 6.0, with K_i from 2 μM to 9 mM (Table 4), while 4-methoxybenzylamine also behaved as a non-competitive

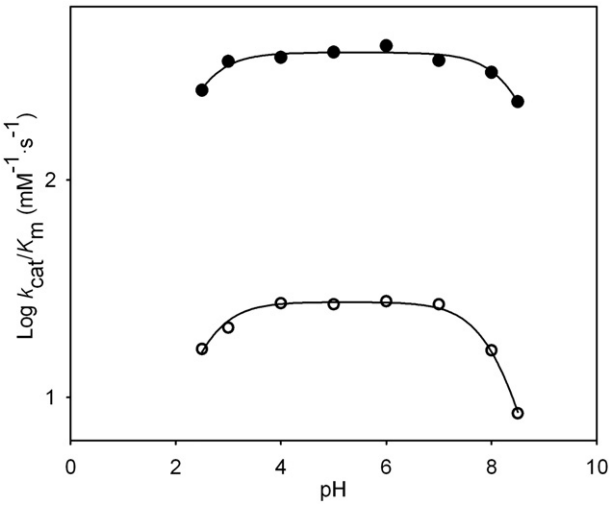

Fig. 5. Effect of pH on oxidase catalytic efficiency on two alcohol substrates. k_{cat}/K_m values for oxidation of *p*-anisyl (–●–) and vanillyl (–○–) alcohols at 24 °C and different pH values. Data were fitted to Eq. 6.

Table 4
Competitive inhibitors of veratryl alcohol oxidation by the new oxidase

		K_i (μM)
Eugenol	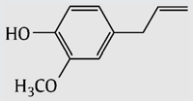	2±0.00009
Benzyl-methyl ether	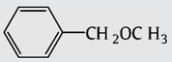	40±1
4-(Methoxymethyl)phenol	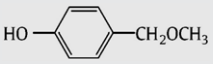	137±9
4-Methoxybenzylamine	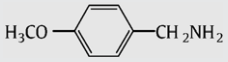	8404±911
Methanol	CH_3OH	172,105±26,273

Inhibition was determined at 24 °C in 100 mM sodium phosphate, pH 6.0.

inhibitor at pH 8.0, with a K_i around 6 mM. Methanol also acted as a competitive inhibitor of veratryl alcohol oxidation but only at very high concentrations (K_i, 172 mM).

4. Discussion

4.1. Fungal oxidases acting on aromatic alcohols

Two well-characterized oxidases of aromatic alcohols have been described up to now. AAO (EC 1.1.3.7), exhaustively characterized in *Pleurotus* species, acts on nonphenolic benzyl alcohols [17,30] while VAO (EC 1.1.3.38), first described in *P. simplicissimum*, oxidizes *p*-hydroxylated benzenic compounds (including alcohols, amines, ethers and alkylphenols) [20,21]. In this study, a new extracellular oxidase was purified and characterized from cultures of an arthroconidial fungus identified as an anamorph of *B. adusta* [25]. Two AAO isoforms have been reported from cultures of *B. adusta* [16], as well as from *Pleurotus sajor-caju* and *Pleurotus floridanus* [12,28], while a unique isoform has been purified from *P. eryngii*, *P. ostreatus* and *Pleurotus pulmonarius* [14,15,17]. However, it was not shown if the two *B. adusta* isoforms resulted from post-translational modification. This seems to be the case in the arthroconidial fungus investigated here, since the two isoelectric focusing bands observed in some samples corresponded to differently glycosylated forms. This glycoprotein shows physicochemical properties similar to those reported for *P. eryngii* AAO, including a monomeric nature and dissociable FAD. By contrast, *P. simplicissimum* VAO is an octamer with covalently-bound FAD. The presence of a FAD cofactor is in agreement with the existence of an ADP-binding motif [33], characteristic of GMC oxidoreductases, whose first residues could be identified in the N-terminus of the new oxidase: ATFFTDASQLPATVYDFIVVG (underlined). This N-terminal region showed the highest identity with the putative AAO from *Postia placenta* (JGI Eukaryotic Genomics project; http://www.genome.jgi-psf.org/Pospl1/Pospl1.home.html) followed by AAO from *P. eryngii*, and glucose oxidase from *A. niger*, among others [34], all of them in the aforementioned family. By contrast, VAO belongs to a different family of FAD oxidoreductases [35]. Another difference between them concerns the ability to stabilize a semiquinone radical intermediate during flavin reduction, which has been shown in VAO but was not demonstrated in the new oxidase and the AAO from *P. eryngii*.

In order to characterize the substrate specificity of the new enzyme, several oxidase substrates were tested (including aromatic alcohols and aldehydes, and some aliphatic alcohols). In the case of benzylic compounds, the effect of different substituents (including methoxy, halogen, hydroxyl and nitro groups) in different positions of the aromatic ring was evaluated as discussed below.

4.2. Oxidation of nonphenolic benzyl alcohols

The oxidase from the *B. adusta* anamorph oxidizes all the nonphenolic substrates reported for *P. eryngii* AAO, including 2,4-hexadien-1-ol in addition to the aromatic benzyl alcohols mentioned below [17,30]. Among them, *p*-anisyl alcohol was the best substrate of both enzymes, showing a similar turnover value that suggests a common oxidation mechanism. The highest activity on *p*-anisyl alcohols is related to the electron-donating nature of the methoxy group, facilitating the electrophilic attack on the benzyl position. The low affinity of the new enzyme for veratryl alcohol, compared with *p*-anisyl alcohol, suggests that the presence of an additional methoxy substituent introduces steric constraints (resulting in a very high K_m value) that does not seem to be so important in *P. eryngii* AAO.

Oxidation of benzyl alcohols, albeit very inefficiently [36,37], has also been reported in some methanol oxidases (EC 1.1.3.13). In addition to some ascomycetous fungi [38,39], these oxidases are produced by wood-rotting basidiomycetes where they represent an H_2O_2 source [7]. However, primary aliphatic alcohols (C_1–C_4) are their preferred substrates in all cases. Methanol was not oxidized by the new oxidase, which is consistent with previous studies on *P. eryngii* AAO [17], and a high concentration (mM range) was required for inhibiting oxidation of aromatic alcohols. Furthermore, the molecular mass (250–700 kDa) and other physicochemical characteristics clearly distinguish methanol oxidases from AAO. The above inhibitory effect of methanol had not been reported in *P. eryngii* AAO (probably because no concentration sufficiently high had been used) [17,30] and shows that a saturated aliphatic alcohol can inhibit aromatic alcohol oxidase activity although only at very high concentrations.

The high catalytic efficiency of the *B. adusta* anamorph oxidase in oxidizing chlorinated benzyl alcohols including *m*-chlorobenzyl alcohol (in spite of the presence of an electron withdrawing substituent) seems to be related to an increased enzyme affinity due to the presence of the chlorine group, since the turnover of *m*-chlorobenzyl alcohol was lower than that of *m*-anisyl alcohol.

The production of mono- and dichlorinated anisyl metabolites has been reported in several *Bjerkandera* strains [40]. In addition to other possible functions, these halogenated compounds could play a role in lignin degradation enabling H_2O_2 production since they are excellent substrates of *Bjerkandera* AAO. It is interesting, from an ecological point of view, that both *Bjerkandera* and *Pleurotus* species secrete into the environment the highest amount of those substituted benzyl alcohols that are the best substrates of the extracellular oxidases they produce, i.e. *p*-anisyl alcohol in the case of *Pleurotus* [3] and 3-chloro-*p*-anisyl alcohol in the case of *Bjerkandera* [2]. In this way, optimal production of the H_2O_2 required for lignin degradation [1] is obtained by redox-cycling of these aromatic metabolites, which would also involve myceliar AAD (EC 1.1.1.90) reducing the aromatic aldehydes formed by AAO [4,31].

4.3. Oxidation of phenolic benzyl alcohols

Phenolic benzyl alcohols are among the typical substrates of VAO, although this enzyme requires the presence of the hydroxyl group at the *p*-position of the benzenic ring to oxidize alcohols to the corresponding aldehydes, and also to catalyze oxidative demethylation, hydroxylation and deamination reactions [20]. The oxidase from the *B. adusta* anamorph, and the *P. eryngii* AAO [30], did not catalyze the latter

reactions, but the corresponding phenolic substrates caused competitive inhibition of veratryl alcohol oxidation. It is interesting that the best VAO substrates described, chavicol and eugenol, are the strongest inhibitors of the *P. eryngii* AAO [30], and the new oxidase, respectively.

We investigated the influence of the phenolic hydroxyl group on the activity of the new oxidase. A substantial reduction of turnover was observed using coniferyl alcohol compared with cinnamyl alcohol. However, the 4-hydroxy substituent did not reduce significantly the turnover for vanillyl alcohol, compared with *m*-anisyl alcohol that was better than some typical AAO substrates tested. Activity on vanillyl alcohol had been previously mentioned in *B. adusta* AAO, but with low levels [16]. Another oxidase from a basidiomycete anamorph, identified as *Geotrichum candidum*, acted similarly on vanillyl alcohol, but poorly on nonphenolic aromatic alcohols [41]. The new oxidase is the first known enzyme that oxidizes both phenolic and nonphenolic benzyl alcohols at significant rates.

As reported for typical AAO [17,30], the new enzyme is optimally active at pH 5.5–6.0 for the oxidation of both *p*-anisyl and vanillyl alcohols. In contrast, VAO acts at basic pH, since the phenolate form is involved in catalysis resulting in a *p*-quinone methide intermediate [42]. Oxidation of vanillyl alcohol by the new oxidase should obey a different mechanism, since it works at slightly acidic pH and deprotonation of the phenolic group at high pH did not increase the rate of aldehyde formation. Most probably this mechanism is the same as that used by this oxidase for oxidation of nonphenolic benzyl alcohols that, as indicated by the k_{cat}/K_m *vs* pH profile for both *p*-anisyl and vanillyl alcohols, suggests the involvement of a histidine residue with a pK_a near 8, as described in glucose oxidase [43]. This residue, corresponding to *A. niger* glucose oxidase His516, is conserved in other GMC oxidoreductases, being His502 in *P. eryngii* AAO [44], and plays a direct role in catalysis, stabilizing the initially reduced flavin anion and the superoxide anion intermediate [45] and promoting hydride transfer from substrate to flavin acting as an active base [46].

4.4. Oxidation of aromatic aldehydes

This study has also revealed that the oxidase from the *B. adusta* anamorph rapidly transforms several aromatic aldehydes to their corresponding acids, exhibiting the highest activity towards aldehydes with halogenated or other electron withdrawing substituents. Although, hydroxy- and methoxy-benzaldehydes have been reported as bad substrates for xanthine oxidase [47], this is the first time that efficient oxidation of both aromatic alcohols and aldehydes is reported in a flavooxidase. Other flavoenzymes catalyze the complete oxidation of alcohol substrates to their corresponding acids, as described for choline oxidase [48].

The enhanced aldehyde oxidase activity in the presence of electron withdrawing substituents is consistent with oxidation of these compounds *via* their *gem*-diol forms as suggested by Ferreira et al. [49] for the *P. eryngii* AAO residual activity on aldehydes [17]. This is also the case for some other GMC oxidoreductases that oxidize aldehydes to their corresponding acids [38,48]. Oxidation of aromatic aldehydes can contribute to peroxide generation, since *Bjerkandera* is able to reduce aromatic acids to their corresponding aldehydes and alcohols [50] closing the redox cycle, as described in *P. eryngii* [4].

4.5. Concluding comments

The new flavooxidase is most probably a member of the GMC oxidoreductase family, as suggested by its biochemical and catalytic properties (including basic pK_a for alcohol oxidation) and N-terminal sequence, associated with the most fully characterized AAO of *P. eryngii*. However, it differs substantially from this enzyme in its ability to efficiently oxidize phenolic alcohols and aromatic aldehydes. In the near future, cloning and sequencing of the corresponding gene will permit the identification of the active-site residues responsible for these new catalytic properties, including the mechanism for hydroxybenzyl alcohol oxidation that differs from that previously described for VAO [42].

Acknowledgements

This study has been supported by the Spanish projects BIO2005-03569, BIO2006-11393, BIO2008-01533 and S-0505/AMB0100 and the BIORENEW European project (NMP2-CT-2006-026456). The authors thank the Instituto de Ciencia de Materiales de Aragón (CSIC, Zaragoza, Spain) for the synthesis of 3-chloro-*p*-anisyl alcohol. E. Romero thanks the Spanish CSIC for an I3P PhD fellowship, and P. Ferreira the EC for a Project Contract.

References

[1] A.T. Martínez, M. Speranza, F.J. Ruiz-Dueñas, P. Ferreira, S. Camarero, F. Guillén, M.J. Martínez, A. Gutiérrez, J.C. del Río, Biodegradation of lignocellulosics: microbiological, chemical and enzymatic aspects of fungal attack to lignin, Intern. Microbiol. 8 (2005) 195–204.
[2] E. de Jong, J.A. Field, J.A.F.M. Dings, J.B.P.A. Wijnberg, J.A.M. de Bont, De novo biosynthesis of chlorinated aromatics by the white-rot fungus *Bjerkandera* sp BOS55. Formation of 3-chloro-anisaldehyde from glucose, FEBS Lett. 305 (1992) 220–224.
[3] A. Gutiérrez, L. Caramelo, A. Prieto, M.J. Martínez, A.T. Martínez, Anisaldehyde production and aryl-alcohol oxidase and dehydrogenase activities in ligninolytic fungi from the genus *Pleurotus*, Appl. Environ. Microbiol. 60 (1994) 1783–1788.
[4] F. Guillén, C.S. Evans, Anisaldehyde and veratraldehyde acting as redox cycling agents for H_2O_2 production by *Pleurotus eryngii*, Appl. Environ. Microbiol. 60 (1994) 2811–2817.
[5] P.J. Kersten, Glyoxal oxidase of *Phanerochaete chrysosporium*: its characterization and activation by lignin peroxidase, Proc. Natl. Acad. Sci. U.S.A. 87 (1990) 2936–2940.
[6] G. Daniel, J. Volc, E. Kubatova, Pyranose oxidase, a major source of H_2O_2 during wood degradation by *Phanerochaete chrysosporium*, *Trametes versicolor*, and *Oudemansiella mucida*, Appl. Environ. Microbiol. 60 (1994) 2524–2532.
[7] G. Daniel, J. Volc, L. Filonova, O. Plihal, E. Kubatova, P. Halada, Characteristics of *Gloeophyllum trabeum* alcohol oxidase, an extracellular source of H_2O_2 in brown rot decay of wood, Appl. Environ. Microbiol. 73 (2007) 6241–6253.
[8] P. Baldrian, V. Valaskova, Degradation of cellulose by basidiomycetous fungi, FEMS Microbiol. Rev. 32 (2008) 501–521.
[9] C.S. Evans, M.V. Dutton, F. Guillén, R.G. Veness, Enzymes and small molecular mass agents involved with lignocellulose degradation, FEMS Microbiol. Rev. 13 (1994) 235–240.
[10] L. Marzullo, R. Cannio, P. Giardina, M.T. Santini, G. Sannia, Veratryl alcohol oxidase from *Pleurotus ostreatus* participates in lignin biodegradation and prevents polymerization of laccase-oxidized substrates, J. Biol. Chem. 270 (1995) 3823–3827.
[11] V.C. Farmer, M.E.K. Henderson, J.D. Russell, Aromatic-alcohol-oxidase activity in the growth medium of *Polystictus versicolor*, Biochem. J. 74 (1960) 257–262.
[12] R. Bourbonnais, M.G. Paice, Veratryl alcohol oxidases from the lignin degrading basidiomycete *Pleurotus sajor-caju*, Biochem. J. 255 (1988) 445–450.
[13] F. Guillén, A.T. Martínez, M.J. Martínez, Production of hydrogen peroxide by aryl-alcohol oxidase from the ligninolytic fungus *Pleurotus eryngii*, Appl. Microbiol. Biotechnol. 32 (1990) 465–469.
[14] G. Sannia, P. Limongi, E. Cocca, F. Buonocore, G. Nitti, P. Giardina, Purification and characterization of a veratryl alcohol oxidase enzyme from the lignin degrading basidiomycete *Pleurotus ostreatus*, Biochim. Biophys. Acta 1073 (1991) 114–119.
[15] E. Varela, B. Böckle, A. Romero, A.T. Martínez, M.J. Martínez, Biochemical characterization, cDNA cloning and protein crystallization of aryl-alcohol oxidase from *Pleurotus pulmonarius*, Biochim. Biophys. Acta 1476 (2000) 129–138.
[16] A. Muheim, R. Waldner, M.S.A. Leisola, A. Fiechter, An extracellular aryl-alcohol oxidase from the white-rot fungus *Bjerkandera adusta*, Enzyme Microb. Technol. 12 (1990) 204–209.
[17] F. Guillén, A.T. Martínez, M.J. Martínez, Substrate specificity and properties of the aryl-alcohol oxidase from the ligninolytic fungus *Pleurotus eryngii*, Eur. J. Biochem. 209 (1992) 603–611.
[18] Y. Asada, A. Watanabe, Y. Ohtsu, M. Kuwahara, Purification and characterization of an aryl-alcohol oxidase from the lignin-degrading basidiomycete *Phanerochaete chrysosporium*, Biosci. Biotechnol. Biochem. 59 (1995) 1339–1341.
[19] M. Goetghebeur, M. Nicolas, S. Brun, P. Galzy, Production and excretion of benzyl alcohol oxidase in *Botrytis cinerea*, Phytochemistry 31 (1992) 413–416.
[20] M.W. Fraaije, C. Veeger, W.J.H. van Berkel, Substrate specificity of flavin-dependent vanillyl-alcohol oxidase from *Penicillium simplicissimum*. Evidence for the production of 4-hydroxycinnamyl alcohols from allylphenols, Eur. J. Biochem. 234 (1995) 271–277.
[21] E. de Jong, W.J.H. van Berkel, R.P. van der Zwan, J.A.M. de Bont, Purification and characterization of vanillyl alcohol oxidase from *Penicillium simplicissimum*. A novel aromatic alcohol oxidase containing covalently bound FAD, Eur. J. Biochem. 208 (1992) 651–657.

[22] A. Mattevi, M.W. Fraaije, A. Mozzarelli, L. Olivi, A. Coda, W.J.H. van Berkel, Crystal structures and inhibitor binding in the octameric flavoenzyme vanillyl-alcohol oxidase: the shape of the active-site cavity controls substrate specificity, Structure 5 (1997) 907–920.
[23] H. Furukawa, M. Wieser, H. Morita, T. Sugio, T. Nagasawa, Purification and characterization of vanillyl-alcohol oxidase from *Byssochlamys fulva* V107, J. Biosci. Bioeng. 87 (1999) 285–290.
[24] J. García-Guinea, V. Cárdenes, A.T. Martínez, M.J. Martínez, Fungal bioturbation paths in a compact disk, Naturwissenschaften 88 (2001) 351–354.
[25] E. Romero, M. Speranza, J. García-Guinea, A.T. Martínez, M.J. Martínez, An anamorph of the white-rot fungus *Bjerkandera adusta* capable of colonizing and degrading compact disc components, FEMS Microbiol. Lett. 275 (2007) 122–129.
[26] N.M. Yoon, C.S. Pak, H.C. Brown, S. Krishnamurthy, T.P. Stocky, Selective reductions. XIX. The rapid reaction of carboxylic acids with borane-tetrahydrofuran. A remarkably convenient procedure for the selective conversion of carboxylic acids to the corresponding alcohols in the presence of other functional groups, J. Org. Chem. 38 (1973) 2786–2792.
[27] Y. Kimura, Y. Asada, M. Kuwahara, Screening of basidiomycetes for lignin peroxidase genes using a DNA probe, Appl. Microbiol. Biotechnol. 32 (1990) 436–442.
[28] A.T. Martínez, S. Camarero, F. Guillén, A. Gutiérrez, C. Muñoz, E. Varela, M.J. Martínez, J.M. Barrasa, K. Ruel, M. Pelayo, Progress in biopulping of non-woody materials: chemical, enzymatic and ultrastructural aspects of wheat-straw delignification with ligninolytic fungi from the genus *Pleurotus*, FEMS Microbiol. Rev. 13 (1994) 265–274.
[29] J.D. Thompson, D.G. Higgins, T.J. Gibson, CLUSTAL W: improving the sensitivity of progressive multiple sequence alignment through sequence weighting, position-specific gap penalties and weight matrix choice. Nucleic Acids Res. 22 (1994) 4673–4680.
[30] P. Ferreira, M. Medina, F. Guillén, M.J. Martínez, W.J.H. van Berkel, A.T. Martínez, Spectral and catalytic properties of aryl-alcohol oxidase, a fungal flavoenzyme acting on polyunsaturated alcohols, Biochem. J. 389 (2005) 731–738.
[31] E. de Jong, A.E. Cazemier, J.A. Field, J.A.M. de Bont, Physiological role of chlorinated aryl alcohols biosynthesized de novo by the white rot fungus *Bjerkandera* sp strain BOS55, Appl. Environ. Microbiol. 60 (1994) 271–277.
[32] A. Hassan-Abdallah, R.C. Bruckner, G.H. Zhao, M.S. Jorns, Biosynthesis of covalently bound flavin: isolation and in vitro flavinylation of the monomeric sarcosine oxidase apoprotein, Biochemistry 44 (2005) 6452–6462.
[33] D.R. Cavener, GMC oxidoreductases. A newly defined family of homologous proteins with diverse catalytic activities, J. Mol. Biol. 223 (1992) 811–814.
[34] E. Varela, M.J. Martínez, A.T. Martínez, Aryl-alcohol oxidase protein sequence: a comparison with glucose oxidase and other FAD oxidoreductases, Biochim. Biophys. Acta 1481 (2000) 202–208.
[35] M.W. Fraaije, W.J.H. van Berkel, J.A.E. Benen, J. Visser, A. Mattevi, A novel oxidoreductase family sharing a conserved FAD-binding domain, Trends Biochem. Sci. 23 (1998) 206–207.
[36] V. Menon, C.T. Hsieh, P.F. Fitzpatrick, Substituted alcohols as mechanistic probes of alcohol oxidase, Bioorg. Chem. 23 (1995) 42–53.
[37] A.K. Kumar, P. Goswami, Functional characterization of alcohol oxidases from *Aspergillus terreus* MTCC 6324, Appl. Microbiol. Biotechnol. 72 (2006) 906–911.
[38] R.N. Patel, C.T. Hou, A.I. Laskin, P. Derelanko, Microbial oxidation of methanol: properties of crystallized alcohol oxidase from a yeast, *Pichia* sp, Arch. Biochem. Biophys. 210 (1981) 481–488.
[39] H.S. Ko, Y. Yokoyama, N. Ohno, M. Okadome, S. Amachi, H. Shinoyama, T. Fujii, Purification and characterization of intracellular and extracellular, thermostable and alkali-tolerant alcohol oxidases produced by a thermophilic fungus, *Thermoascus aurantiacus* NBRC 31693, J. Biosci. Bioeng. 99 (2005) 348–353.
[40] H.E. Spinnler, E. de Jong, G. Mauvais, E. Semon, J.-L. Le Quéré, Production of halogenated compounds by *Bjerkandera adusta*, Appl. Microbiol. Biotechnol. 42 (1994) 212–221.
[41] S.J. Kim, N. Suzuki, Y. Uematsu, M. Shoda, Characterization of aryl alcohol oxidase produced by dye-decolorizing fungus, *Geotrichum candidum* Dec1, J. Biosci. Bioeng. 91 (2001) 166–172.
[42] M.W. Fraaije, W.J.H. van Berkel, Catalytic mechanisms of the oxidative demethoxylation of 4-(methoxymethyl)phenol by vanillyl-alcohol oxidase. Evidence for formation of a p-quinone methide intermediate, J. Biol. Chem. 272 (1997) 18111–18116.
[43] J.P. Roth, J.P. Klinman, Catalysis of electron transfer during activation of O_2 by the flavoprotein glucose oxidase, Proc. Natl. Acad. Sci. U.S.A. 100 (2003) 62–67.
[44] P. Ferreira, F.J. Ruiz-Dueñas, M.J. Martínez, W.J.H. van Berkel, A.T. Martínez, Site-directed mutagenesis of selected residues at the active site of aryl-alcohol oxidase, an H2O2-producing ligninolytic enzyme, FEBS J. 273 (2006) 4878–4888.
[45] J.P. Klinman, How do enzymes activate oxygen without inactivating themselves? Acc. Chem. Res. 40 (2007) 325–333.
[46] G. Wohlfahrt, S. Trivic, J. Zeremski, D. Pericin, V. Leskovac, The chemical mechanism of action of glucose oxidase from *Aspergillus niger*, Mol. Cell Biochem. 260 (2004) 69–83.
[47] G.I. Panoutsopoulos, C. Beedham, Kinetics and specificity of guinea pig liver aldehyde oxidase and bovine milk xanthine oxidase towards substituted benzaldehydes, Acta Biochim. Pol. 51 (2004) 649–663.
[48] F. Fan, M.W. Germann, G. Gadda, Mechanistic studies of choline oxidase with betaine aldehyde and its isosteric analogue 3,3-dimethylbutyraldehyde, Biochemistry 45 (2006) 1979–1986.
[49] P. Ferreira, M.J. Martínez, J. Jiménez-Barbero, A.T. Martínez, B. Herguedas, M. Medina, Catalytic mechanisms of aryl-alcohol oxidase from *Pleurotus eryngii*, Proc. 16th Inter. Symp. Flavins and Flavoproteins, Jaca, 9–12 June, 2008.
[50] A. Hage, H.E. Schoemaker, J.A. Field, Reduction of aryl acids by white-rot fungi for the biocatalytic production of aryl aldehydes and alcohols, Appl. Microbiol. Biotechnol. 52 (1999) 834–838.